

# Dolomitization and silicification in low-energy lacustrine carbonates (Paleogene, Madrid Basin, Spain)

M.A. Bustillo <sup>a,\*</sup>, M.E. Arribas <sup>b</sup>, M. Bustillo <sup>b</sup>

<sup>a</sup>*Dpto. de Geología, Museo Nacional de Ciencias Naturales, CSIC, José Gutiérrez Abascal 2, Madrid 28006, Spain*

<sup>b</sup>*Dpto. de Petrología y Geoquímica, Facultad de Ciencias Geológicas, Universidad Complutense, Madrid 28040, Spain*

---

## Abstract

Repetitive sequences of carbonate deposits, occurrence include in the lower part of the Paleogene Carbonate Unit (northeast border of the Madrid Basin), have been studied, defining regressive lacustrine sequences and early diagenetic processes. Binocular microscopic examination, scanning electron microscopic/energy dispersive X-ray observations, and X-ray diffraction analyses joint to isotopic studies ( $\delta^{18}\text{O}$  and  $\delta^{13}\text{C}$ ) have been used to characterise the facies and environments. The sequences consist of a lower uncemented carbonate mud unit, calcitic or dolomitic in composition, and an upper carbonate unit (arenites, bioclastic limestones, and microbial laminated limestones with cherts). Visual features (vertical prismatic structures, fissures, massive nodulization, rhizoliths, brecciation) and microscopic features (micrite micronodules, vug porosity, circumgranular cementation, gypsum lenticular crystals) outline pedogenic processes. These features, found locally in bioclastic and microbial laminated limestones or in dolomite uncemented muds, define, respectively, palustrine limestones or dolocretes. Facies analysis allows us to define several lacustrine sub-environments (basinal, littoral, eulittoral and supralittoral) and characterises different types of shallowing upward lacustrine sequences, either with or without subaerial exposure. The isotopic values of the bioclastic and microbial laminated limestone (from  $-5.77\text{‰}$  to  $-6.78\text{‰}$  for  $\delta^{13}\text{C}$ , and from  $-5.25\text{‰}$  to  $-5.53\text{‰}$  for  $\delta^{18}\text{O}$ ) and those of uncemented calcitic muds (from  $-5.80\text{‰}$  to  $-7.01\text{‰}$  for  $\delta^{13}\text{C}$ , and from  $-4.98\text{‰}$  to  $-5.58\text{‰}$  for  $\delta^{18}\text{O}$ ) establish that both types of carbonates precipitated in equilibrium with meteoric waters. In the palustrine carbonate deposits, the  $\delta^{13}\text{C}$  values suggest a strong organic contribution. The dolomitization that only affected the uncemented carbonate muds is early interpreted because of the structural and compositional characteristics of the dolomite (micro-rhombic dolomicrite, nearly stoichiometric and poorly ordered), and because the calculated average  $\Delta^{18}\text{O}_{\text{dol-cal}}$  for calcitic and dolomitic uncemented muds is about  $6\text{‰}$ . The  $\delta^{18}\text{O}$  isotopic values indicate that the dolomite precipitated from water that was slightly more enriched in heavy isotopes than the calcite, because of an increase in evaporation rates. Nodules and nodular levels of cherts occur in the upper units of littoral and eulittoral sequences, probably as a consequence of the existence of microbial mats that could include the silica source. According to their mineralogy (Opal CT and quartz/moganite) and structures (double nodules, lamination and bioturbation), three types of chert are described (TB, MB and WO). These types define three general stages of silicification during the early diagenesis, from the recently buried to the postcompaction of carbonate deposits. The  $\delta^{18}\text{O}$  values of quartz show that the silicification and ageing of opaline phases occurred from meteoric waters, which were lighter than the calcite or

---

\* Corresponding author. Fax: +34-91-564-4740.

*E-mail addresses:* abustillo@mncn.csic.es (M.A. Bustillo), earribas@eucmax.sim.ucm.es (M.E. Arribas), bustillo@eucmax.sim.ucm.es (M. Bustillo).

dolomite precipitating waters. The cherts included in palustrine limestones show  $\delta^{18}\text{O}$  values of quartz that record more evaporated waters than those of the general stages of silicification.

**Keywords:** Shallow lacustrine carbonates; Chalks; Dolomitization; Cherts; Paleogene; Madrid Basin

---

## 1. Introduction

In shallow and marginal lacustrine environments, relatively small changes in lake level can impact greatly on the depositional regimes. When such areas are subject to episodic subaerial exposure, several pedogenic changes also take place (Freytet and Plaziat, 1982). As a result, a great variation of facies, along with complex lateral and vertical changes, is frequent, making facies-sequence analysis very difficult and sometimes impossible (Tucker and Wright, 1990; Platt and Wright, 1991). In low-energy lakes, carbonates are formed under intense biological activity, and in such cases, the meteoric and diagenetic transformations that the primary sediments suffer are both specific and considerable (Platt and Wright, 1991). Our study focuses on the different Paleogene lacustrine carbonate sequences formed in shallow and marginal environments in low-energy lakes. The studied sequences are unusual in that they display uncemented carbonate muds together with indurated carbonates containing cherts.

Silicification is a significant diagenetic phenomenon of ancient carbonate rocks because the cherts, formed by it, shed light upon many aspects of the diagenetic history of the carbonate host rocks. The silica concentration of the pore fluids, the chemical environment of the silicification, and the relative timing of the silicification with respect to the other diagenetic events that affect the carbonate host rocks can be ascertained (Hesse, 1990).

The Paleogene carbonate deposits of the Madrid Basin are an interesting example of the above as they display sections with many, and successive, similar sequences. These repetitive sequences make it possible to study the local variations of carbonate sedimentation together with the different chert types and dolomitization. The purpose of this paper is: (i) to describe the sedimentary realms, analysing the palustrine and lacustrine carbonate facies and their association in sequences, and (ii) to document the changes that the

limestones underwent and to explain the formation of confined diagenetic facies that include dolomites and chert.

## 2. Geological setting

The Madrid Basin (Fig. 1A) is located in central Spain. It is a foreland basin formed during the compressive phase of the Alpine build-up, which also caused the formation of the Iberian Range and the Central System. The Central System is included in the Hesperian Massif hosting low to high-rank metamorphic rocks. The Iberian Range is a mountain belt with a double vergence and developed from a depositional trough of the aulacogen type filled with mesozoic deposits within the Iberian plate (Alvaro et al., 1979). The fill of the Madrid basin comprises Paleogene and Neogene terrestrial deposits. Paleogene deposits are scattered along the northeast border of the Madrid Basin (Fig. 1B) and are synorogenic with the Alpine orogeny. Paleogene outcrops are nearest to the area of convergence between the Iberian Range and the Central System (Fig. 1A). In this area, the greater part of the Paleogene deposits consists of carbonate and detrital rocks, which occurs within a succession formed by two lithological units: Carbonate and Detrital Units (Arribas, 1986a,b, 1994) (Fig. 2). These units are apparently conformable above an evaporitic unit that is also possibly Paleogene in age. The sediments reflect an evolution from a lacustrine environment (Carbonate Unit) to one of the prograding alluvial fans (Detrital Unit) sourced from the Central System and Iberian Range (Arribas and Arribas, 1991). The base of this Paleogene succession is partially covered and eroded. The lower part of the succession contains a faunal association of macro- and micro-mammals indicating a late Eocene Headonian age (Arribas et al., 1983).

One of the best exposures of these Paleogene sediments occurs in the locality of Torremocha de Jadraque (Fig. 2B) (Guadalajara province). In this area, the

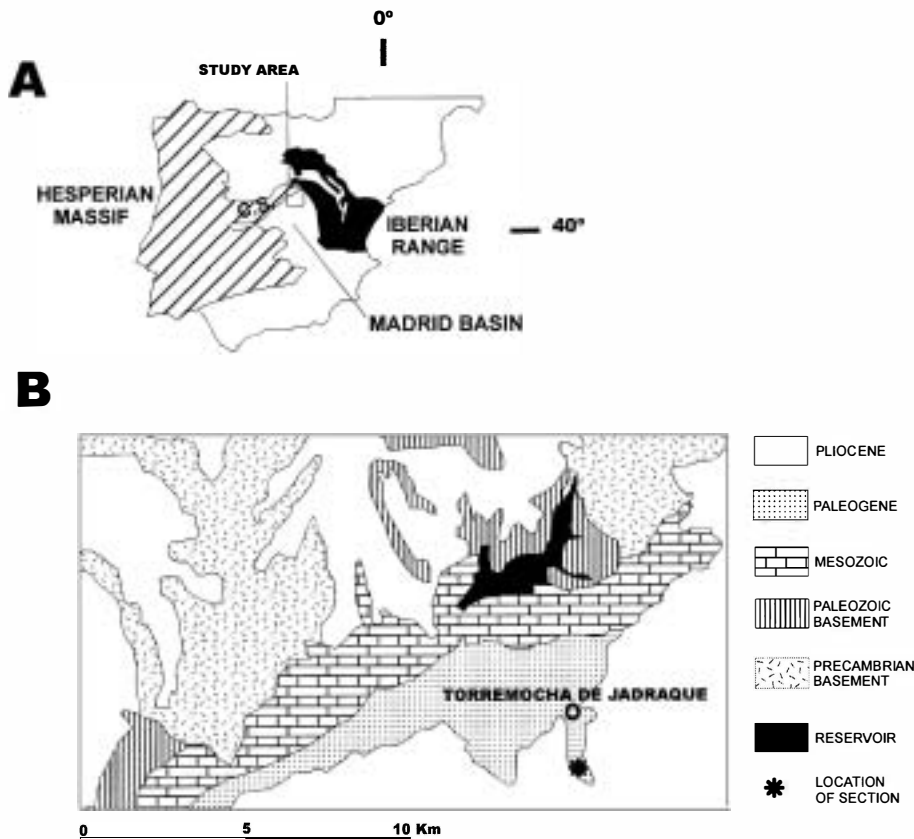


Fig. 1. Geological setting of the study area. (A) Distribution of the Hesperian massif, Iberian Range and Madrid Basin in the Iberian Peninsula. C.S., Central System. (B) Geological map of the study area and location of the studied stratigraphic section.

Paleogene succession has a maximum thickness of 880 m. The carbonate unit, with a thickness of 510 m, contains a variety of carbonate facies interpreted as deposits of a lacustrine environment (Arribas, 1986a). In this study, a section at the middle of the Torremocha de Jadraque exposure is analysed (Fig. 2). The studied section is formed by many sequences where uncemented carbonate (calcitic or dolomitic) muds are overlaid by limestones that frequently contain cherts. Along the Carbonate Unit, lacustrine sandstones also appear as sediments related to the alluvial fan progradation (Arribas, 1986b). The sandstones are mainly lithoarenites in composition (Arribas and Arribas, 1991), composed exclusively of carbonates (limestones and dolostones) derived from Mesozoic rocks of the Iberian Range.

### 3. Sampling and analytical study

The sampling strategy was to collect several samples from the sequences defined by an upper carbonate indurated unit and a lower soft unit (uncemented carbonate muds). The general mineralogy, the type of calcite, the proportion of  $\text{CaCO}_3$  to dolomite and the degree of ordering of the dolomite was determined by X-ray diffraction (Hardy and Tucker, 1988).

Textures and mineralogy were studied with a polarised light microscope and a scanning electron microscope (SEM, Philips KL-20) equipped with an energy dispersive X-ray analyser (EDAX-DX-4i). Trace-element determinations were made by ICP-MS in the Chemical Laboratory of the University of Granada. After  $\text{HNO}_3 + \text{HF}$  digestion of 0.1000 g of

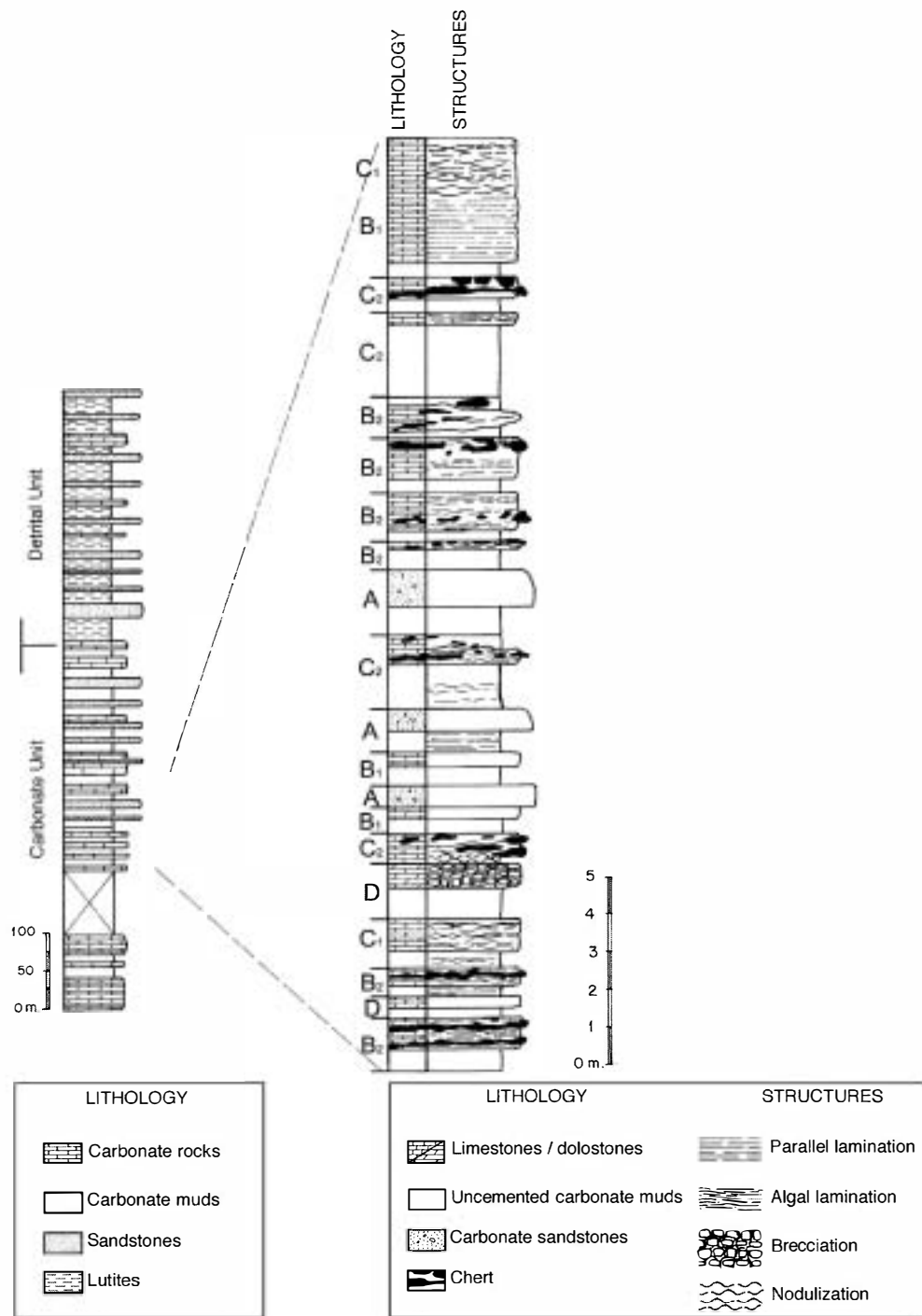


Fig. 2. Paleogene general section and studied section in the surroundings of Torremocha de Jadraque (A, B, etc., are the type of sequence of Fig. 8).

sample powder in a Teflon-lined vessel at  $\sim 180^\circ\text{C}$  and  $\sim 200$  p.s.i for 30 min, evaporation to dryness, and subsequent dissolution in 100 ml of 4 vol.%  $\text{HNO}_3$ . Instrument measurements were carried out in triplicate with a PE SCIEX ELAN-5000 spectrometer using Rh as internal standard. Precision was greater than  $\pm 2\%$  and  $\pm 5\%$  for concentrations of 50 and 5 ppm, respectively.

Isotope measurements were carried out in the Stable Isotope Laboratory at the University of Salamanca. Carbon dioxide was evolved from the carbonates using 103% phosphoric acid for 3 h (calcite) or 24 h (dolomite) in a thermostatic bath at  $25^\circ\text{C}$  (McCrea, 1950). Some calcites were analysed using an ISOCARB device at  $90^\circ\text{C}$ . Oxygen from the cherts was extracted using the method of Clayton and Mayeda (1963), but employing a loading technique as described by Friedman and Gleason (1973) and  $\text{ClF}_3$  as reagent (Borthwick and Harmon, 1982). Isotopic ratios were measured in a Micromass SIRA-II mass spectrometer. Overall precision, including extraction is  $\pm 0.1\text{‰}$  for  $\delta^{13}\text{C}$  and  $\pm 0.06\text{‰}$  for  $\delta^{18}\text{O}$  in carbonates, and  $\pm 0.2\text{‰}$  for fluorination. The values obtained for relevant standards are: for NBS-19,  $\delta^{13}\text{C}=2.00\text{‰}$ ,  $\delta^{18}\text{O}=-28.86\text{‰}$ , and for NBS-28,  $\delta^{18}\text{O}=9.6\text{‰}$ . Delta values take into account corrections derived from the contribution of mass 17 to the  $\delta^{18}\text{O}$  values (Craig, 1957).

## 4. Petrology and sedimentology

### 4.1. Carbonate facies

#### 4.1.1. Uncemented carbonate muds

These facies are porous, massive carbonates and form the lower units in the sequences (Fig. 2). They constitute beds from 0.5 to 1 m thick, and high porosities are maintained in spite of the age and the depth of burial. They consist of calcite, dolomite or mixtures of both. Two types of facies have been defined: calcitic and dolomitic.

The calcitic muds contain more than 90% calcite (LMC, with 2–4 mol%  $\text{MgCO}_3$ ). Under SEM, these muds are micrites comprising subhedral crystals, sometimes with rhombic shapes, measuring up to  $10\text{ }\mu\text{m}$  and with a high intercrystalline porosity (Fig. 3a and b). Charophyte and ostracod fragments may be present in

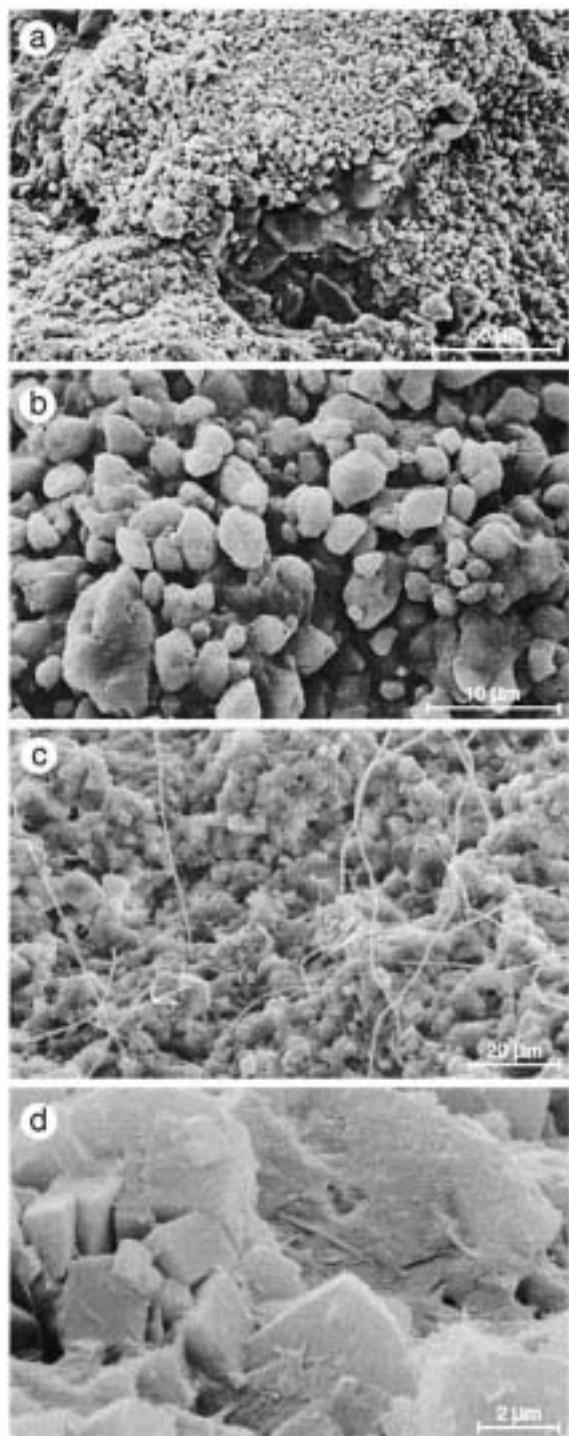
small proportions ( $<2\%$ ). The calcitic muds display a low clay minerals content ( $<10\%$ ). These clay particles are Al-smectite, illite, palygorskite and sporadic sepiolite (Bustillo et al., 1998). Under thin section, pedogenic features, such as a circumgranular porosity and micritic micronodules, are observed. Calcitic cementation only occurs locally (Fig. 3c).

The dolomitic muds have different mixtures of calcite and dolomite with up to 90% of dolomite. Under SEM, these muds are dolomicrites consisting of euhedral dolomite rhombohedra ( $<7\text{ }\mu\text{m}$  in size) (Fig. 3c) with a high intercrystalline and intracrystalline porosity (hollow crystals). Locally, the dolomite crystals can be re-covered by palygorskite (Fig. 3d). The dolomite is nearly stoichiometric, with 49.00–50.65 mol%  $\text{CaCO}_3$  (calculated by Lumsden, 1979 equation) and poorly ordered (0.37–0.48), the highest values corresponding to samples with dolomitic extrabasinal grains. The euhedral dolomite crystals are locally enclosed in large calcite crystals, as a consequence of a local and later calcitic cementation. The dolomitic muds have a low content (10–15%) in clay minerals (mainly illite, Al-smectite and palygorskite).

When dolomitic muds are overlain by lacustrine carbonate sandstones, a high percentage of dolomite occurs, as extrabasinal grains together with other extrabasinal grains occur. In extrabasinal dolomite grains, the surfaces of the dolomite crystals show corrosion and dissolution.

#### 4.1.2. Carbonate sandstones

Carbonate sandstones are interbedded with the carbonate muds. These facies constitute sheets from 0.5 to 0.8 m thick and erosional surfaces at the bottom are not present. Bioclasts are absent and a massive structure and some parallel lamination are common features. Petrographic analysis of these sandstones reveals a high percentage of extrabasinal carbonate grains. These sandstones have been classified as sedarenites according to Zuffa (1980). The greater part of extrabasinal carbonate grains has a dolomitic composition and the principal textures of each grain are dolospartic mosaic and monocrystalline. Minor calcitic rock fragments have also been recognised (mudstone with echinoids, wackestones and bioclastic grainstones). These sandstones have been interpreted as the first clastic input-related to alluvial fan deltas developed in the lacustrine basin (Arribas, 1986b). The structural, textural and



compositional features are indicative of deposition from the decanting of fine clastic sediments into the most distal parts of the lacustrine littoral, as fine deltaic sheets.

#### 4.1.3. Bioclastic limestones

These carbonates form metre-thick beds with a massive structure, and they sometimes show parallel lamination. They are mudstones and wackestones with charophytes, molluscs, ostracod fragments and cyanobacterial filament remains.

#### 4.1.4. Microbial laminated limestones

These limestones constitute beds of 0.5–1.3 m thick. They are abundant in the stratigraphic section and they show, under polished thin-sections, an irregular and parallel biolamination. Laminae are composed of clotted micrite with a biotic association of limnic organisms: cyanobacterial filament remains, charophyte and ostracod fragments. Silicification is common in these facies.

#### 4.1.5. Palustrine limestones

Palustrine limestones (Fig. 4a and b) occur as metre-thick beds in which several pedogenic features can be recognised: massive nodulization, rhizoliths, and brecciation. These palustrine limestones are superimposed on bioclastic limestones and microbial laminated limestones (Fig. 4a). Locally, silicification effects are present with complex chert nodules. Carbonate microfabrics and other features of subaerial exposure included grainification (micritic micronodules formation), vuggy porosity, circumgranular cementation and development of lenticular gypsum crystals, now pseudomorphed by calcite (100–200 μm in size). Under SEM, they display a micritic texture and occasionally palygorskite fibres occupying an intercrystalline microporosity. Charophyte and ostracod fragments and cyanobacteria filaments appear as relics.

Fig. 3. SEM pictures of uncemented carbonate muds. (a) Calcitic muds. The micrites with subhedral crystals and high intercrystalline porosity locally show cements of larger calcite crystals. (b) High-magnification view of (a), where the shape and size of calcite crystals can be observed. (c) Dolomitic muds with small euhedral dolomite crystals. Modern biological filaments must not be considered. (d) Detail of the (c) where palygorskite fibres occur on the dolomite crystals.

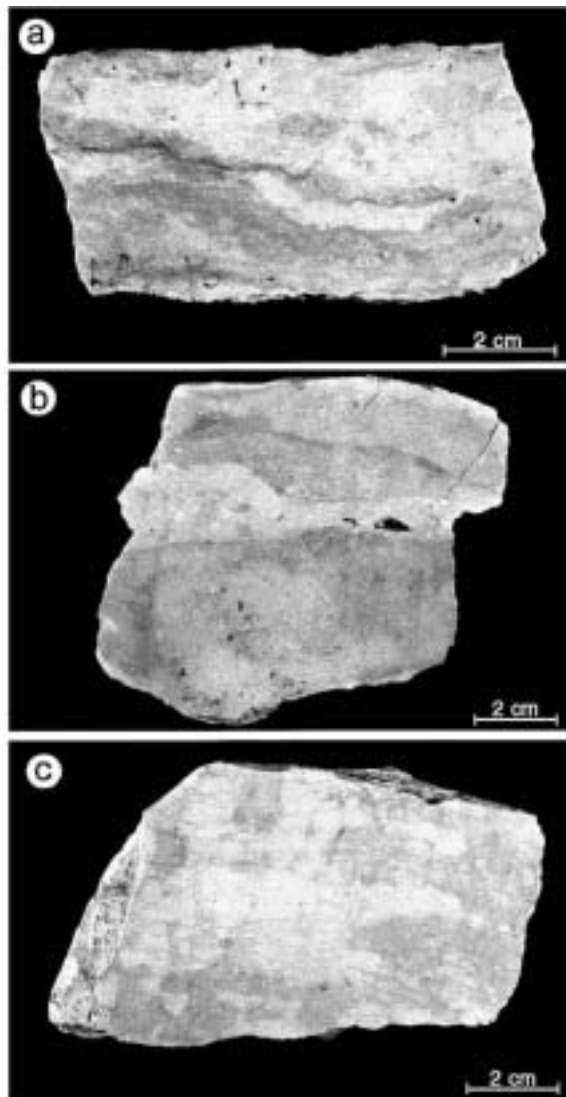


Fig. 4. Hand specimen photographs of several indurated carbonate facies. (a) Palustrine limestone with irregular lamination (possibility microbial) affected by pedogenesis. (b) Micritic micronodules and vug porosity in a palustrine limestone. (c) Dolocrete showing brecciation due to desiccation processes.

#### 4.1.6. Dolocrete

Only two dolocrete levels have been distinguished. They are between 0.1 and 0.5 m in thickness, and are located at the base of the studied section. They are overprinted on dolomitic muds. They are massive and lack any fossils. They show vertical joint planes on their upper surfaces. Polished sections show skew

planes with horizontal and oblique planar fissuring (Fig. 4c). All these features are due to desiccation processes. Under thin section, they display micrite texture, and SEM images reveal dolomites with a high degree of intercrystalline microporosity occupied, sometimes, by palygorskite fibres.

#### 4.2. Chert types

Cherts only appear in the microbial laminated limestones and in the palustrine limestones, forming isolated nodules and nodular levels along all the beds. They are complex in mineralogy, fabric and structure (Fig. 5), being sometimes made up of two juxtaposed nodular shapes (double nodules) (Fig. 5a, b, c, d and f). Taking into consideration their colour and translucency, three different types have been defined.

##### 4.2.1. Translucent brown or cream chert (TB chert)

These cherts appear as nodules with sharp and toothed edges. In the double nodules, the translucent chert is located in the centre and is enveloped by the matt brown chert (Fig. 5a and b). Mineralogical relics of the host-rocks are scarce but this chert can show many vertical millimetric bioturbation channels (Fig. 5a and b). Although the present carbonate host-rock displays a discontinuous laminated, or lenticular, structure, it does not appear in this chert.

Under light microscopy, the groundmass of the TB chert consists largely of a mosaic of little anhedral quartz crystals (less than 20  $\mu\text{m}$  size) and length-fast chalcedony (Fig. 6a and b, TB part) and has no mineralogical relics of the host rock. Void-filling phases include length-fast chalcedony and megaquartz and they enhance the bioturbation channels. Megaquartz appears only as a result of the silicification of the fragments of ostracods, charophytes and microbial mat remains. Under SEM, these cherts are very compact and it is difficult to observe the crystals, but sometimes small silica microspheres, calcite and palygorskite can be observed.

This type of chert, when it is included in palustrine limestones, can show a white cortex (Fig. 5e), which replaces and breaks the nodule. This cortex is formed by large euhedral or anhedral calcite crystals (Fig. 6c), locally replaced by megaquartz, microquartz and different types of length slow chalcedony (quartzine and lutecite).

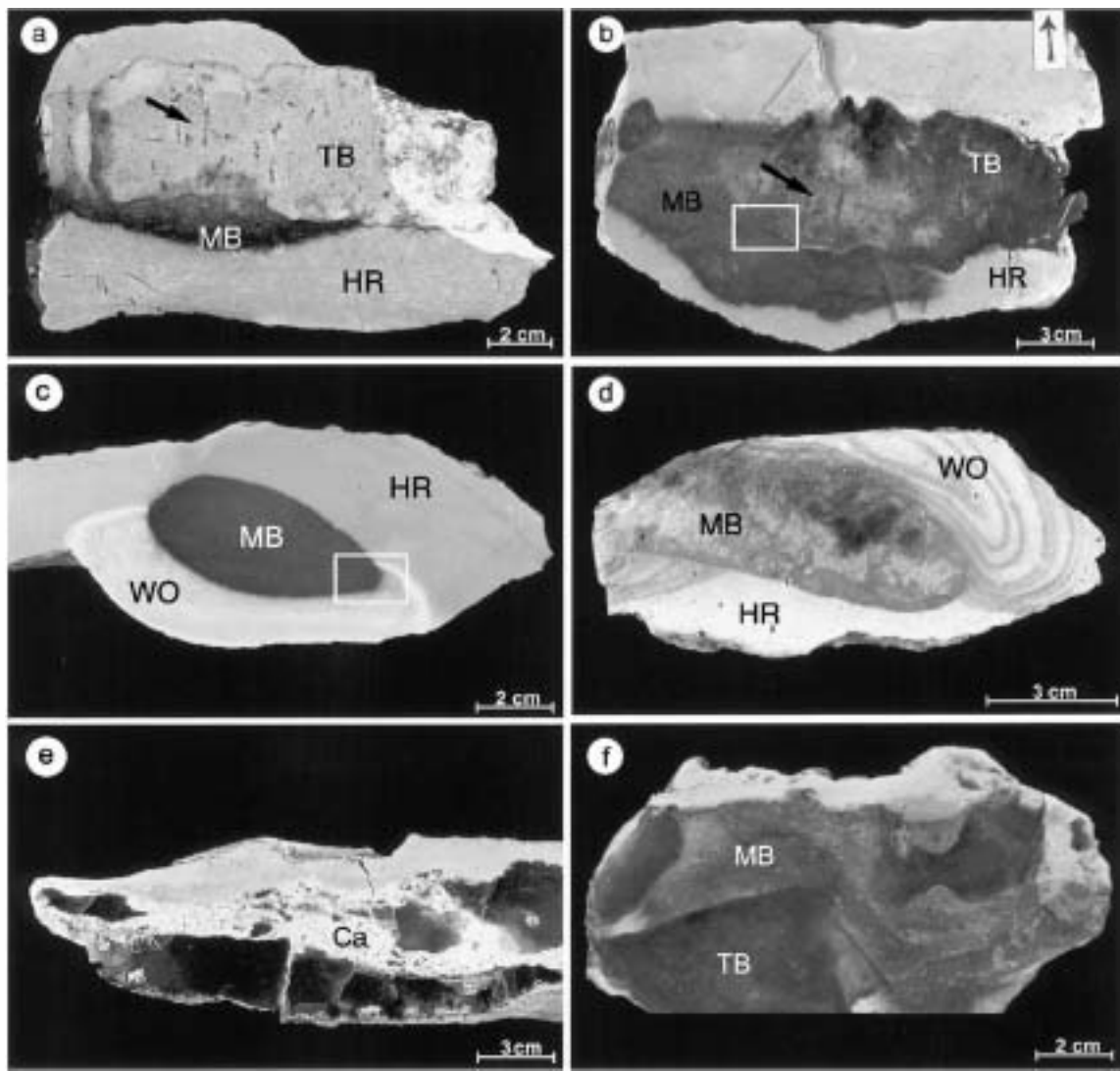


Fig. 5. Hand specimen photographs of chert nodules. (a) Double nodule formed by TB chert (upper) and MB chert (lower). MB chert grows after TB chert and reproduces the same discontinuous lenticular lamination as the present host rock (HR). TB chert shows millimetric vertical bioturbation channels (arrow) that do not occur neither in MB chert nor in the host rock (HR). (b) Double nodule where TB chert is partially enveloped by MB chert. TB chert, with some bioturbation channels (arrow), maintains sharp contact with the host rock. MB chert displays diffuse contact with the host rock reproducing its lenticular structure. The square contains the area seen in (a and b). (c) Double nodule with an inner part of MB chert and an outer part of WO chert. The square contains the area seen in (e). (d) MB chert partially enveloped by WO chert that display Liesegang structures. The WO chert is deformed by compaction on MB chert because is opaline. (e) TB chert nodule in palustrine limestone. Some parts of the chert have a white carbonate cortex that break and replace the nodule. (f) Double nodule where it can be seen that the lamination of the MB chert is adapted to TB chert.

X-ray powder diffractometer patterns of the TB chert show an atypical quartz. The ratio of intensities of the 101 peak to the 100 peak for the quartz is high (around 7), and the pattern shows weak peaks at the  $d$ -

spacing around 4.45, 3.11 and 2.86 Å, that correspond to the moganite (Bustillo, 2001). The crystallinity index of quartz (Murata and Norman, 1976) is low and ranges between 1 and 2.

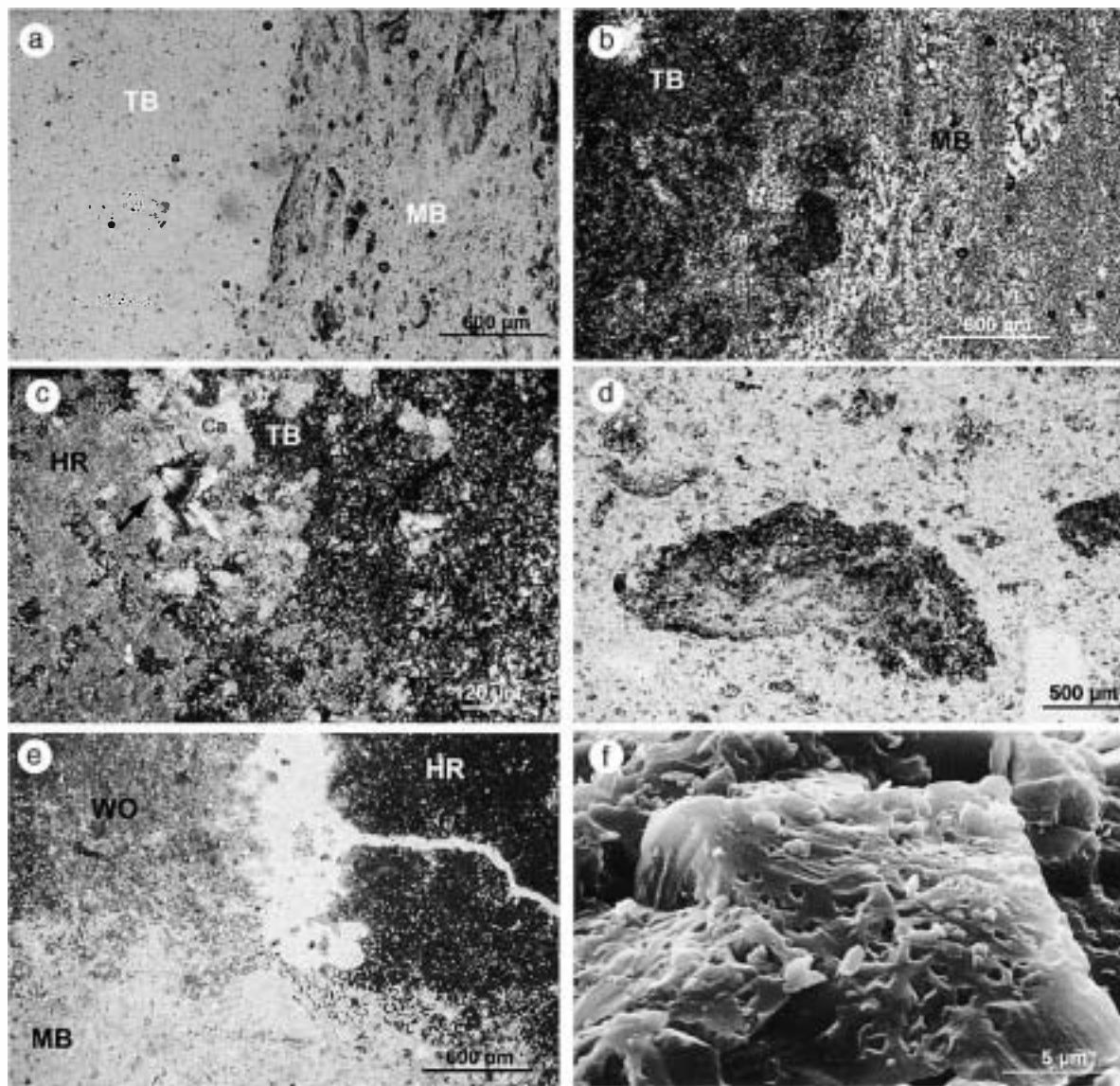


Fig. 6. Thin sections and SEM pictures of cherts. (a) TB chert (left) in contact with MB chert (right) (see Fig. 4b). TB chert does not present host rock relics and MB chert displays parallel host rock relics. Plane-polarized light. (b) TB chert has very small quartz crystals while MB chert has larger crystals. A parallel lamination is only observed in MB chert. Crossed nicols. (c) White cortex in Fig. 4e. Large calcite crystals replace the TB chert and some of these crystals are later replaced by length-slow chalcedony (arrow). Crossed nicols. (d) Undetermined algae buildings included in MB chert. Plane-polarized light. (e) Contact zone between MB chert, WO chert and host rock (square zone in Fig. 4c). The numerous, tiny and white spheroids in the host rock (HR) are the island of advance in the attack front of the MB chert and these are maintained in the opal (WO chert) formed during the following silicification. Plane-polarized light. (f) SEM view of the quartz crystals in the MB chert. The large quartz crystal includes numerous small calcite crystals or moulds of them.

#### 4.2.2. Matt brown chert (MB chert)

This chert has diffused edges with the host rocks. It displays the same structure as that of carbonate host

rock and includes many relics of it. In the double nodules, the MB chert envelops the TB chert (Fig. 5a and b) or is enveloped by the white opaline chert,

depending on the levels (Fig. 5c and d). In the first case, the lamination recorded in MB adapts to the shape of TB chert (Fig. 5f). Under light microscopy, the MB chert consists of mosaic quartz, where most of the crystals (between 20 and 100  $\mu\text{m}$  size) are larger than those of TB chert (Fig. 6a and b, MB part). As well as the large relics of the host rock (Fig. 6d) included in the MB chert, the quartz crystals of this type of chert enclose tiny calcite inclusions. “Islands of advance” (Grigor’ev, 1965) appear in the attack front with the carbonate host-rock (Fig. 6e), and these “islands” are maintained when this type of chert is enveloped by the opaline white chert (W $\bullet$ ). Under SEM, the groundmass shows megaquartz crystals with small euhedral calcite crystal inclusions (between 1 and 3  $\mu\text{m}$ ) or hollows left by them (Fig. 6f). Occasionally, microbial relics of the host rocks can be observed.

X-ray powder diffractometer patterns of the MB chert are typical and show the presence of quartz and variable amounts of calcite. The ratio of intensities of the 101 peak to the 100 peak for the quartz is normal (around 5) and the index of crystallinity is high (around 7). The calcite included in the chert is low-magnesium calcite, like that of the host rock.

#### 4.2.3. White opaline chert (W $\bullet$ chert)

This chert appears at the upper part of the section as single nodules or double nodules where it grows on MB chert (Fig. 5c and d). Locally, the nodules can be altered, appearing as powdery nodules. The contact with their host rocks is sharp and sometimes the white opaline cherts present Liesegang structure (Fig. 5d). This chert reflects the different structures of the present host rocks. The groundmass of this chert consists of opal, which is partially recrystallized to microcrystalline quartz at some points. Length-fast chalcedony and megaquartz are mainly found in the replacement of microfossils and in cements. The opal, which is semi-isotropic under thin section, sometimes displays silica microspheres under SEM. Small amounts of Mg were detected with EDAX.

X-ray powder diffractometer patterns of this chert show the presence of opal CT, quartz and sometimes calcite. The pattern of the quartz cannot be compared with those obtained in the other types of chert because of the interference of opal. The opal CT displays a low

degree of ordering (4.08–4.11 for the cristobalite peak).

## 5. Geochemistry

### 5.1. Isotope Geochemistry

Oxygen and carbon isotopic analyses were performed on 19 selected carbonate samples (calcite and/or dolomite) covering different types of carbonate facies, from palustrine to lacustrine carbonates (Table 1) (Fig. 7). Oxygen isotopic analyses were also carried out on chert samples (Table 2).

#### 5.1.1. Lacustrine and pedogenic carbonates

Carbon and oxygen stable isotopic values lie close to those of average fresh water carbonates (Keith and Weber, 1964; Hudson, 1977). Although non-marine environments usually have wide variations of stable

Table 1  
Isotopic composition of the carbonate samples

Sample	Type of carbonate	$\delta^{13}\text{C}$ ‰PDB	$\delta^{18}\text{O}$ ‰PDB
MAE-2	BALL	−5.77	−5.25
MAE-21	BALL	−6.78	−5.46
MAE-26A	BALL	−6.49	−5.53
MAE-3	CUM	−6.41	−5.58
MAE-18	CUM	−7.01	−5.38
MAE-36	CUM	−5.80	−4.98
MAE-4	DUM	−4.10	−0.65
MAE-14	DUM	−3.75	+0.70
MAE-30	DUM	−4.37	+1.24
MAE-5	DUM-DF	−3.40	−0.82
MAE-5	DUM-CF	−5.30	−4.25
MAE-20	DUM-DF	−2.80	−1.44
MAE-20	DUM-CF	−6.05	−4.63
MAE-11	PL	−6.60	−6.01
MAE-26B	PL	−7.16	−5.47
MAE-34C	PL	−6.25	−5.17
MAE-2	CHR	−4.74	−4.20
MAE-26	LC	−7.25	−9.04
MAE-34	CHR	−5.74	−4.14

BALL — Bioclastic and microbial laminated limestone.

CUM — Calcitic uncemented mud.

DUM — Dolomitic uncemented mud.

DUM-DF — Dolomitic uncemented mud, dolomite fraction.

DUM-CF — Dolomitic uncemented mud, calcite fraction.

PL — Palustrine limestones.

CHR — Relics of carbonate host rock in chert.

LC — Later calcite in chert.

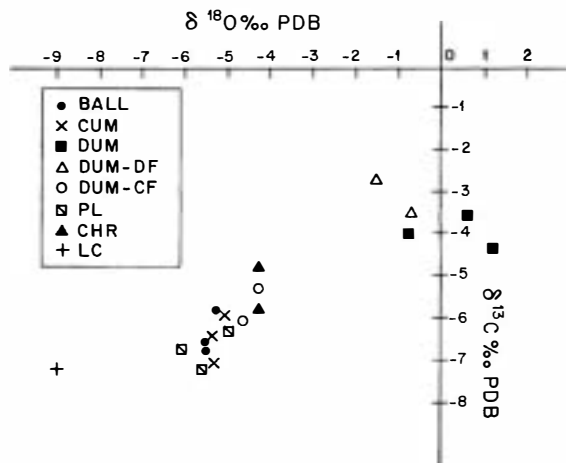


Fig. 7.  $\delta^{18}\text{O}$  vs.  $\delta^{13}\text{C}$  for lacustrine and palustrine carbonates.

isotope values (Talbot and Kelts, 1990; Casanova and Hillaire-Marcel, 1992; Camoin et al., 1997), the results for the studied carbonates indicate considerable isotopic homogeneity (Table 1) (Fig. 7).

The bioclastic and microbial laminated limestone data vary from  $-5.77\text{‰}$  to  $-6.78\text{‰}$  for  $\delta^{13}\text{C}$  and from  $-5.25\text{‰}$  to  $-5.53\text{‰}$  for  $\delta^{18}\text{O}$ . The values for calcitic uncemented muds range from  $-5.80\text{‰}$  to  $-7.01\text{‰}$  for  $\delta^{13}\text{C}$  and from  $-4.98\text{‰}$  to  $-5.58\text{‰}$  for  $\delta^{18}\text{O}$ . The narrow  $\delta^{18}\text{O}$  range (Fig. 7) suggests that these types of carbonates formed, in a broad sense, under similar conditions of water input and climatic environment. The palustrine limestones have very similar isotopic compositions, ranging from  $-6.25\text{‰}$  up to  $-7.16\text{‰}$  for  $\delta^{13}\text{C}$  and from  $-5.17\text{‰}$  up to  $-6.01\text{‰}$  for  $\delta^{18}\text{O}$  (Table 2). These values lie close to pedogenic carbonates of Talma and Netterberg (1983).

The dolomitic uncemented muds, which only consist of dolomite (samples MAE-4, MAE-14 and MAE-30 in Table 1), have  $\delta^{13}\text{C}$  values ranging from  $-3.75\text{‰}$  to  $-4.37\text{‰}$  and  $\delta^{18}\text{O}$  values from  $-0.65\text{‰}$  to  $1.24\text{‰}$ . Those with mixtures of calcite and dolomite (samples MAE-5 and MAE-20 in Table 2) display differences. The values of the dolomite fraction vary from  $-3.40\text{‰}$  to  $-2.80\text{‰}$  for  $\delta^{13}\text{C}$  and from  $-0.82\text{‰}$  to  $-1.44\text{‰}$  for  $\delta^{18}\text{O}$ . The values of the calcite fraction vary from  $-5.30\text{‰}$  to  $-6.05\text{‰}$  for  $\delta^{13}\text{C}$  and from  $-4.25\text{‰}$  to  $-4.63\text{‰}$  for  $\delta^{18}\text{O}$ . Thus, the calcite fraction in mixed samples is more enriched in  $^{18}\text{O}$  than the calcite in samples, formed only of this mineral, and the dolomite fraction is more enriched in  $^{16}\text{O}$  than the dolomite in samples, formed exclusively of this mineral.

### 5.1.2. Cherts

The isotopic study of the cherts is carried out from two points of view: carbon and oxygen isotope composition of the host rocks relics and other calcites included in the chert (Table 1) and the oxygen isotope composition of the silica phases (Table 2).

The carbon and oxygen isotope composition of the carbonate relics is quite similar (samples MAE-2 and MAE-34 in Table 1) to those obtained in their host rocks, indicating that silicification does not affect the composition of the included carbonates. However, the later big euhedral or anhedral calcite crystals that replace the chert present different values that are very light (sample MAE-26 in Table 1).

In the double nodules, the oxygen isotope composition of quartz in the TB part and in the MB part (samples MAE-2 and TJ-4) is almost identical. Assuming that the quartz precipitated in near-surface

Table 2  
Isotopic composition of chert

Description	Location	Sample and Chert type	$\delta^{18}\text{O}$ SMOW (quartz)
Double nodule	Base of section	MAE-2 TB	+28.7
TB (first) and MB (second)		MAE-2 MB	+28.8
Double nodule	Base of section	TJ-4 TB	+29.5
TB (first) and MB (second)		TJ-4 MB	+29.8
Single nodule	Medium	MAE-26 TB	+30.9
Double nodule	Top of section	MAE-34 MB	+27.0
MB (first) and WO (second)		MAE-34 WO	+25.6
Double nodule	Top of section	MAE-35 MB	+26.8
MB (first) and WO (second)		MAE-35 WO	+28.6

conditions with temperatures of 15–20 °C, the isotopic values for the TB and MB parts, ranging between +28.7‰ and +29.8‰ (SMOW), and reveal a  $\delta^{18}\text{O}$  of the water from which they precipitated between –10‰ and –8‰ (SMOW) (Clayton et al., 1972). The chert in palustrine limestone that shows several reversible replacements (sample MA-26 in Table 2) present quartz with the highest isotopic value, around 30.9‰ (SMOW), corresponding this situation to more evaporitic formation waters (–5‰, SMOW).

Finally, the W opaline chert samples (samples MAE-34 and MAE-35) show very different oxygen isotope values, 25.6‰ and 28.6‰, respectively. These values must not be considered here for discussion, since these types of cherts contain an important percentage of opal and then the hydroxyl ions or the water may erroneously yield light  $\delta^{18}\text{O}$  values (Kolodny and Epstein, 1976; Matheney and Knauth, 1993; McBride et al., 1999).

## 5.2. Elemental geochemistry

The results obtained in shallow and basinal lacustrine carbonates are shown in Table 3. We analysed only Mg/Ca and Sr/Ca ratios because these ratios in the inorganic calcite can be a useful tool to interpret the environment salinity of the lake (Gasse et al., 1987). These authors, studying Holocene lakes in North Sahara, find periods of low salinity in lake waters when the Sr/Ca mol ratio of the inorganic calcite varies from 0.00164 to 0.00221 and the Mg/Ca ranges from 0.0313 to 0.0416. In the studied samples, Mg/Ca mol ratio ranges from 0.0155 to 0.0310 and Sr/Ca varies from 0.00025 to 0.00064. The comparison between the previous authors' data and our data clearly suggests a formation of the studied carbonates from lake waters of

low salinity. This conclusion is consistent with the stable isotope study described above.

## 6. Interpretation

### 6.1. Types of sequences and the sedimentary realms

The carbonate facies are ordered in sequences, which show the evolution of the lacustrine sedimentation (Fig. 8). The base consists of uncemented carbonate muds, often dolomitic, gaining a larger proportion of calcite upwards. The upper units are limestones (limestones with bioclasts, microbial laminated limestones and palustrine limestones) and occasionally dolocretes and sandstones.

The vertical succession of facies indicates regressive sequences in low-energy lakes with low gradient ramp-type margins (Platt and Wright, 1991). According to Gierlowski-Kordesch and Kelts (1994), we can distinguish various sedimentary regimes in lacustrine depositional systems: basinal, littoral, eulittoral and supralittoral (Fig. 8).

#### 6.1.1. Basinal (sequences A, (Fig. 8))

The lower units are uncemented carbonate muds and the upper units are lacustrine sandstones. The uncemented carbonate muds are considered as basinal lacustrine deposits formed in those areas most distal to the littoral of the lake (see discussion in Section 6.3). These sequences are intercalated between other carbonate lacustrine–palustrine sequences. They represent the sedimentation in the basinal areas of the lake with a dominance in clastic sediments.

#### 6.1.2. Littoral (sequences B1 and B2, (Fig. 8))

In sequences B1, upper units are bioclastic with charophytes (stems and gyrogonites) and ostracods, while in sequences B2, upper units are microbial laminated carbonates. Bioclastic limestones are interpreted as shallow-water limestones being the result of a lacustrine sedimentation below water level in littoral realms (Arribas, 1986b). Microbial laminated limestones were interpreted as stromatolites formed below the water level in littoral realms (Arribas, 1986b). Studies of modern analogues of stromatolites indicate that benthic cyanobacteria are often the primary producers of the stromatolite laminae (Chafetz, 1994;

Table 3  
Ca, Mg, and Sr composition and Sr/Ca and Mg/Ca ratios in limestone samples

Sample	Ca (%)	Mg (%)	Sr (ppm)	Sr/Ca (molal)	Mg/Ca (molal)
MAE-2	35.18	0.33	338	0.00044	0.0155
MAE-3	36.51	0.53	202	0.00025	0.0239
MAE-18	36.10	0.68	340	0.00043	0.0310
MAE-21	37.56	0.54	419	0.00051	0.0237
MAE-26	36.77	0.49	342	0.00042	0.0219
MAE-36	35.32	0.70	496	0.00064	0.0326

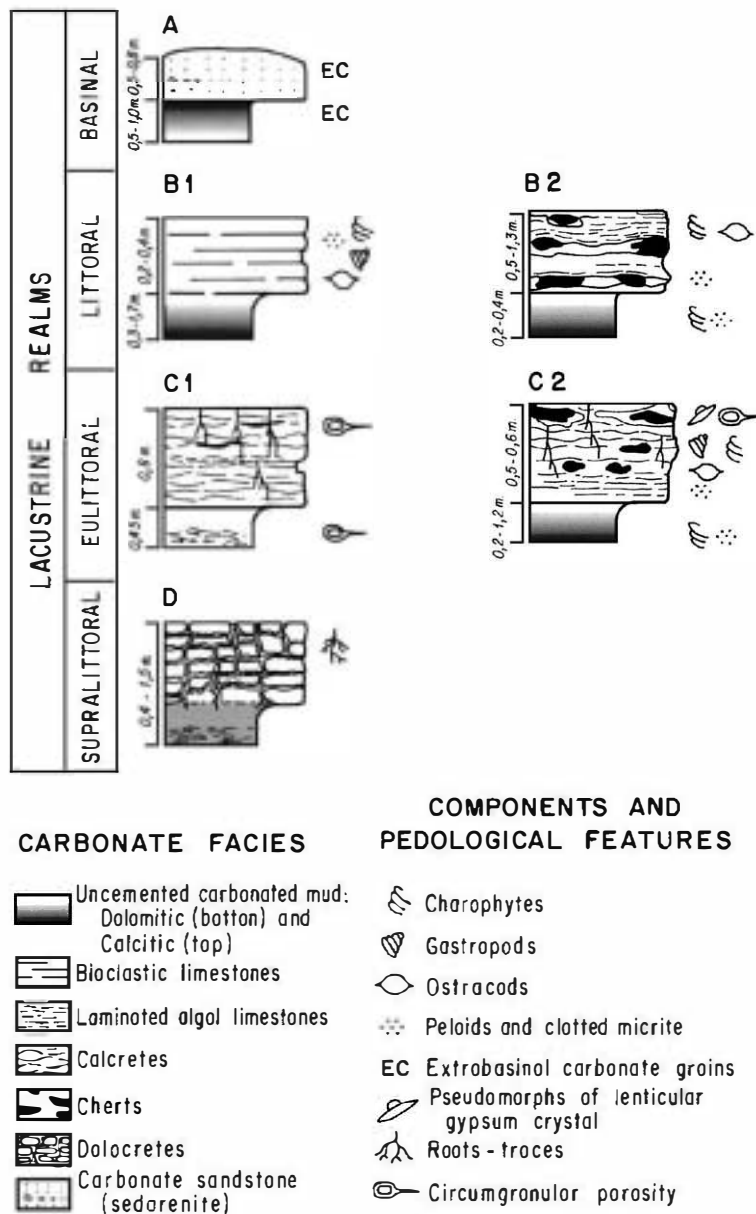


Fig. 8. Carbonate facies, sequences and sedimentary environments.

Gerdes et al., 1994). In these cases, biogenic lamination is the result of precipitate carbonate induced by microbial activity of a complex community of cyanobacteria and diatoms (Gerdes et al., 1994). There, bioclastic limestones and microbial laminated limestones represent stable carbonate sedimentation in the littoral lacustrine realm.

The B1 and B2 sequences are shallowing upward sequences without subaerial exposure.

### 6.1.3. Eulittoral (sequences C1 and C2, (Fig. 8))

These sequences are formed when several subaerial exposure processes have developed on littoral carbonate

nate sediments (bioclastic limestones and microbial laminated limestones) modifying their primary structures and forming palustrine limestones. As it occurs in the preceding sequence, the uncemented muds represent the most distal carbonate sediments in the lacustrine basin. Massive nodulization, rhizoliths, circumgranular cementation, grainification, palygorskite fibre formation and other pedological features indicate that the littoral sediments were textural and structurally modified by subaerial exposure as a result of fluctuations in the water table of the lake. The presence of subaerial exposure features on littoral deposits and the presence of palygorskite fibres indicate periodic fluctuations of the water level in the lake (Freytet and Plaziat, 1982; Platt and Wright, 1991) and characterise a palustrine realm. Sequences C1 and C2 are interpreted as shallowing upward lacustrine sequences with subaerial exposure.

#### 6.1.4. Supralittoral (sequences D, (Fig. 8))

These sequences are very scarce, and dolocretes are superimposed on dolomitic uncemented muds. The occurrence of dolomitic muds and palygorskite suggests a chemical sedimentation from ephemeral lakes enriched in magnesium under semiarid climate and developed in the supralittoral areas. Later, a sudden fall in the water table could have provoked subaerial exposure of the dolomitic muds and dolocrete formation (Bustillo et al., 1998).

### 6.2. Isotopic composition of palustrine and lacustrine limestones

The calcite deposits of all sequences present a narrow range of  $\delta^{18}\text{O}$  values, and therefore it can be deduced that the environmental characteristics of the lake did not change significantly during the successive episodes of carbonate precipitation. The correlation between the  $\delta^{18}\text{O}$  and  $\delta^{13}\text{C}$  values in littoral limestones (non-palustrine) and calcite uncemented muds ( $r=0.72$ ), shows a concomitant enrichment both in  $^{18}\text{O}$  and  $^{13}\text{C}$  of the calcite and, therefore, of the palaeolake water. This may indicate that the calcite precipitated from water with relatively long residence times in systems closed, in a hydrological sense, the recharge-evaporation budget having controlled the isotopic evolution of the water (Talbot, 1990; Talbot and Kelts, 1990).

The  $\delta^{18}\text{O}$  values of water in isotopic equilibrium with the calcites range between  $-3.5\text{‰}$  and  $-5.8\text{‰}$  (SMOW) at surface temperatures (Epstein et al., 1953; Craig, 1965). The low  $\delta^{18}\text{O}$  contents of the calcites indicate the input of  $^{16}\text{O}$ -enriched waters of meteoric origin (Craig and Gordon, 1965; Hudson, 1977), containing isotopically light  $\text{CO}_2$  derived from soils (Spiker, 1980). Such an interpretation can explain the low  $\delta^{13}\text{C}$  values of the samples. Therefore, the data suggest that the lacustrine carbonates precipitated in equilibrium with isotopically light, meteoric waters.

In calcretes, Talma and Netterberg (1983) show an average of about  $-4\text{‰}$  for  $\delta^{13}\text{C}$  measurements globally, although the values can range from  $-12$  to  $+4\text{‰}$ . The lower values indicate oxidation of continental organic matter and/or influence of soil-derived  $\text{CO}_2$ . Since  $\text{C}_3$  or  $\text{C}_4$  plants would produce isotopically less negative values than the soil-derived  $\text{CO}_2$ , and our samples do not display very low  $\delta^{13}\text{C}$  values. The palustrine limestones may have well formed where decaying organic matter provide a very significant source of carbon.

Related to  $\delta^{18}\text{O}$  values, Talma and Netterberg (1983) obtained values for calcretes ranging from  $-9\text{‰}$  to  $+3\text{‰}$ , with an average of about  $-5\text{‰}$ . This last value is approximately the same as that in our palustrine limestones. Higher values, not present in our samples, would reflect a degree of  $\delta^{18}\text{O}$  enrichment due to evaporation processes. Talma and Netterberg (1983) comment that in arid zones,  $\delta^{18}\text{O}$  values of less than  $-5\text{‰}$  do not occur at all. Therefore, the studied palustrine limestones can be considered to have formed in a semiarid zone, with annual rainfall  $>250\text{ mm}$ . In this sense, some authors point out that the parent carbonate in the substrate (lacustrine carbonate) could influence the isotopic signature of the palustrine carbonate (Allan and Matthews, 1982), although the others (e.g. Salomons and Mook, 1976; Salomons et al., 1978) only consider evaporation and  $\text{CO}_2$ -loss to be important.

### 6.3. The uncemented carbonate muds and the dolomitization

Uncemented carbonate muds are very rare sediments in lacustrine environments and are similar in appearance to European chalks (Upper Cretaceous). Generally, chalks are uncemented marine sediments

formed by the deposition of very fine calcitic components (coccoliths, planktonic foraminifera and calcispheres) in pelagic environments. Krenmayr (1997) mentions "freshwater chalks" to characterise uncemented carbonate muds in lacustrine environment. We considered "chalk" as an inappropriate term, where the uncemented carbonates are only crystals and do not show microfossils, as is our case.

Few authors have described uncemented carbonate muds in lacustrine environments and they are usually interpreted as the result of: (i) inorganic precipitation of LMC or HMC in the most distal areas of the lakes (Yévenes et al., 1973; Müller and Wagner, 1978; Arribas and Bustillo, 1985; Krenmayr, 1997), (ii) calcareous plankton ooze in larger lakes (Eugster and Kelts, 1983) and (iii) accumulation of fine detrital carbonates when the source rocks are carbonate rocks (Kelts and Hsü, 1978; Geyh et al., 1971). In the studied uncemented carbonate muds, the absence of microfossils and of detrital features seems to indicate that they are inorganic primary sediments.

In the studied Paleogene carbonate muds, the variation of the mineralogical composition (calcitic and dolomitic) would indicate periodic changes in the hydrochemical composition of the lake water, which influenced the mineralogy of the primary mud (LMC or HMC). In lakes with low salinities, LMC is the most frequent carbonate mineral, while the presence of dolomite suggests a high Mg/Ca ratio (Müller et al., 1972). There are two possible origins for the dolomitic mud: a primary origin from lake waters with a Mg/Ca ratio between 7 and 12 and a secondary origin from the replacement (dolomitization). The characteristics of the early diagenetic or primary dolomite are similar. Lumsden and Chimahusky (1980) suggest that stoichiometric dolomite is the evidence of evaporite-related dolomicrite deposition (early diagenetic or primary origin). In an overview of modern occurrences of dolomite, Last (1990) points out that it is normally poorly ordered, being deposited directly from the lake water or from interstitial pore water. Gunatilaka (1991) invokes a primary origin for recent dolomites showing some degree of disorder and very small sizes (2–5  $\mu\text{m}$ ). Then, in our case, the similarity of porosities between the calcitic and dolomitic muds, and the fact that the dolomite is stoichiometric, micro-rhombic and poorly ordered indicates early diagenetic replacement. The precursor can be metastable, such as

HMC, or stable-like LMC, although an HMC mud is in general more probable.

Uncemented dolomitic sediments in recent lacustrine sediments of Central Spain have been described as the result of an early dolomitization process of HMC mud in basinal realms (Yévenes et al., 1973). Wright et al. (1997) also suggests an HMC mud precursor for Miocene lacustrine micrites in the Madrid Basin. According to these authors, a high intercrystalline and intracrystalline porosity occurs during the replacement process. Considering HMC as the most probable precursor, the formation of HMC lacustrine muds only in some sequences implies chemical changes in the lake waters during the different sequences. These changes are due to a significant increase in evaporation, with salinity changes or an increase in the Mg/Ca ratio (HMC is precipitated in waters with a Mg/Ca ratio of 2–12; Müller et al., 1972).

Using the isotopic composition of dolomite as an indicator of its genesis is not easy because of the uncertainties about the relationship between temperature,  $\delta^{18}\text{O}$  of water and  $\delta^{18}\text{O}$  of dolomite (Tucker and Wright, 1990), and the absence of agreement in the experimental studies of  $\Delta^{18}\text{O}_{\text{dol}-\text{cal}}$  (Degens and Epstein, 1964; Fritz and Smith, 1970; Matthews and Katz, 1977; Land, 1983; among others). Dolomite, in a general sense, is enriched in  $\delta^{18}\text{O}$  in relation to calcite by between +1‰ and +7‰, and is possibly not constant (Neil and Epstein, 1966; Fontes et al., 1970; Land, 1980; Tucker and Wright, 1990). However, McKenzie (1981) suggests that a value of  $\Delta^{18}\text{O}_{\text{dol}-\text{cal}}$  of +2‰ to +4‰ would indicate secondary replacement dolomite in isotopic equilibrium with coexisting calcite and higher fractionation values ( $\Delta^{18}\text{O}_{\text{dol}-\text{cal}}$  from +4‰ to +7‰) could indicate primary dolomite, precipitated according to an ideal dolomite–water isotopic fractionation (Epstein et al., 1964; Neil and Epstein, 1966; Northrop and Clayton, 1966).

According to our data (Table 1), the calculated average  $\Delta^{18}\text{O}_{\text{dol}-\text{cal}}$  for calcitic and dolomitic uncemented muds is about 6‰, which would indicate a primary or early diagenetic origin of the dolomites. If we assume that the calcites and dolomites precipitated at normal surface temperatures (15–25 °C), the  $\delta^{18}\text{O}$  values of water in isotopic equilibrium with the calcites could have range between –3.5‰ and –5.8‰ (SMOW) (Epstein et al., 1953; Craig, 1965), whereas the  $\delta^{18}\text{O}$  values of water in isotopic equilibrium with

the dolomites could have ranged between  $-1.9\%$  and  $-4.1\%$  (SMOW). It suggests that the dolomites precipitated more from evaporated lake water. In other words, the waters from which dolomite precipitated were enriched in heavy isotopes due to an increase of evaporation rates.

#### 6.4. Silicification

The degree of silica supersaturation of the pore waters during the general replacement of the limestones, is responsible for the three types of chert with their different quartz textures and the presence or absence of opal in the groundmass (Maliva and Siever, 1988). The quartz textures found in the cements, and in replaced microbial fragments, only define local microenvironments and cannot be considered in general deductions. After the general replacements, a maturation process (ageing) increased the quartz content at the expense of the opal, and therefore the cherts of the lower part of the section are solely made up of quartz.

The TB chert, with a groundmass composed only of microcrystalline quartz, could have had an opaline precursor. The main argument for the existence of opaline precursors is the presence of small quartz crystals (less than  $10\text{ }\mu\text{m}$ ) and small silica microspheres in the groundmass (Maliva and Siever, 1988). In these cherts, which are the oldest of the section, the maturation process is over and there are no relics of the initial opaline phases. The MB chert is composed of quartz crystals that are large, homogeneous in size, and display calcite inclusions, which shows that this quartz had relatively low nucleation rates and precipitated in pore waters with low degrees of silica supersaturation.

The W● chert, which is rich in opal and shows microcrystalline quartz in the groundmass, is a different case, and it would have been produced from very rich silica solutions. The coexistence of opal and quartz could be explained if an earlier stage of opal-CT precipitation was followed by another one with quartz precipitation, because the silica concentration dropped below opal-CT saturation after the opal precipitation (Maliva and Siever, 1988). However, it is also probable that part of the opaline phases initially precipitated were recrystallized to microcrystalline quartz (ageing).

##### 6.4.1. Stages of silicification

The double nodules determine the two stages of silicification in the limestones. The silica precipitated during the first stage provided the sites for the later silica precipitation as it happens in some silica rhizoliths (Jones et al., 1998).

In the double nodules at the base of the section, MB chert encloses TB chert. Sometimes the structure of the TB chert marks a primary vertical bioturbation (not observed in the present carbonate host rock (Fig. 5a and b), while the structure of MB chert shows the same discontinuous lamination as that of the host rock. Due to the fact that the structures of the present host rock do not coincide with that of the TB chert, we think that the present structure of the host rock was acquired after the first silicification (TB chert). In the host rock, compaction enhanced the microbial lamination and produced a discontinuous, parallel or lenticular, lamination with reorientation of grains. The silicified zone did not acquire this internal structure (orientation of grains or lenticular structure) acquired by the carbonate sediment. Then, the TB chert was formed by an early silicification of the initial bioturbated carbonate sediment and the MB chert, however, was formed by silicification after slight burial and compaction of the host rock. Another fact that indicates that the TB chert pre-dates the MB is that the lamination recorded in MB is adapted to the shape of TB chert (Fig. 5f).

Considering quartz textures, the solutions of the early silicification (TB chert) were richer in silica than those of the second silicification (MB chert). Since the oxygen isotope composition of quartz in the TB chert and in the MB chert is alike, the waters of the replacements and of the ageing of the opaline precursor must have been similar. The values of the water from which quartz precipitated are clearly lighter than the values for the calcite/dolomite precipitating waters shown above. Therefore, the reacting fluid that precipitated the quartz was enriched in isotopically lighter water compared to that in which the calcite precipitated. MB chert is the only type that appears along all the section, and its  $^{15}\text{N}$  isotopic values indicate that the fluids were probably more concentrated in the bottom and evolved to more enriched in isotopically lighter waters to the top.

The time of the first silicification can be deduced from the sequences that finish with palustrine limestones and include TB chert. In these sequences, the quartz of the outer part of the chert nodules is replaced

by calcite. This replacement probably occurred when the host rock was affected by pedogenic processes, as it happens in other continental sequences (Armenteros et al., 1995). The very light values of  $\delta^{18}\text{O}$  ( $-9.04\text{‰}$ ) suggest a telogenetic environment of formation for the calcite crystals. If all this is assumed, this chert was formed before the emergence of the sequence.

At the top of the section, double nodules consist of MB chert partially enveloped by W chert (Fig. 5b and c). The attack front (megaquartz islands of advance) of the MB chert remains visible in the W chert (Fig. 6e). Therefore, W chert was formed later than MB chert from dissolutions richer in silica because opaline minerals were precipitated. The compaction structures of host rocks reflected in both cherts are similar, which shows that both silicifications are produced by the postcompaction of the host rocks. Moreover, the deformation of some opaline nodules, which appear flattened in relation to the MB chert, indicates that the compaction had not been finished when the W chert was formed. The  $^{18}\text{O}$  isotopic composition of the replacement waters from W chert cannot be deduced because the opal amount is high.

#### 6.4.2. Source of silica

The source of silica is not clear, because siliceous microfossils have not been detected in the limestones or in the uncemented carbonate muds. The location of the chert nodules only in the limestones can suggest that the silica source was included only in these facies, because it is difficult to think of a general distribution of silica from the groundwater where the most porous facies have not been affected. The chalks are, in general, very appropriate host rocks for silicification because of their porosity/permeability (Ziljstra, 1995).

The existence of the remains of microbial films in the limestones can explain the presence of silica because such films may provide the loci for silica precipitation. Although they have not been observed, diatoms could have been associated with microbial mats. Riding (1994) and Winsborough (2000) point out that the diatoms appear to be of particular importance in the formation of microbial films, because of their ecological success and their effect on mat growth, stability and trapping. Differences in the grade of dissolution of the frustules, according to the diatom species, can be a hypothesis to explain the liberation of silica in different stages.

## 7. Conclusions

(1) The lower part of the Paleogene Carbonate Unit is formed by carbonate facies that indicate low-energy lakes with low gradient ramp-type margins. Textures and composition allowed us to distinguish several sedimentary carbonate facies, which represent different lacustrine environments: supralittoral, eulittoral, littoral and basinal. These carbonate facies form different types of regressive sequences where calcitic and dolomitic uncemented muds are followed by bioclastic mudstones/wackestones or microbial laminated limestones. When these upper facies of the sequences are affected by subaerial exposure, palustrine limestones and dolocretes complete the shallow-ing upward sequences.

Carbon and oxygen stable isotopic values for littoral (bioclastic mudstones/wackestones and microbial laminated limestones) and basinal lacustrine sediments (uncemented carbonate muds) suggest that both types of carbonates precipitated in equilibrium with meteoric waters, isotopically light. In the palustrine carbonates, the  $\delta^{13}\text{C}$  data outline a strong organic contribution to the dissolved carbon reservoir, probably derived from  $\text{C}_3$  and/or  $\text{C}_4$  plant decay. These conditions do not change significantly for the successive sequences. The correlation between the  $\delta^{18}\text{O}$  and  $\delta^{13}\text{C}$  values in both littoral and basinal lacustrine carbonates may indicate precipitation from water with relatively long residence times in closed systems from a hydrological point of view, being the recharge-evaporation budget which controls the isotopic evolution of the water.

(2) Dolomitization affected only the uncemented carbonate muds and later some of the dolomites then formed were affected by a calcite cementation. The micro-rhombic crystals with poorly ordered and the nearly stoichiometric characteristics and their porosity, similar to the calcitic muds, could indicate an early process. Dolomitic uncemented mud is probably the "end member" of an early dolomitization process overprinting an HMC mud precursor.

Since the calculated average of  $\Delta^{18}\text{O}_{\text{dol-cal}}$  for calcitic and dolomitic uncemented muds is about  $6\text{‰}$ , an early diagenetic origin for the dolomites might also be deduced. If we assume that calcite and dolomite precipitated at normal surface temperatures, the dolomites precipitated from water was more

enriched in heavy isotopes ( $\delta^{18}\text{O}$  values from  $-1.9\text{‰}$  to  $-4.1\text{‰}$  SMOW) than the calcite ( $-3.5\text{‰}$  to  $-5.8\text{‰}$  SMOW) due to an increase of evaporation rates.

(3) The replacement of the limestones by silica only occurs in littoral and eulittoral sequences, probably due to the presence of microbial mats (including diatoms). Three stages of silicification during the early diagenesis and different types of chert are found. The first stage (TB chert) took place before significant burial of the carbonate deposits and the other two stages (MT chert and WO chert) were after the compaction of the limestones. Every stage of silicification was produced from porewaters of different silica supersaturation. According to the quartz textures and the presence or absence of opal CT, the solutions of the first and third stage of silicification were richer in silica than those of the second silicification.

$\delta^{18}\text{O}$  values of quartz in the TB and MB cherts indicate that the formation of quartz in the first and second silicification occurred from similar meteoric waters (from  $-10\text{‰}$  to  $-8\text{‰}$  SMOW), which are clearly lighter than the values for the calcite precipitating waters. Some cherts included in the palustrine limestones are special cases because they record more evaporated waters than those of the general stages of silicification. The isotopic composition of the waters of the third stage of silicification cannot be defined due to the interference of important amounts of opal mixed with quartz in the composition of the WO chert.

## Acknowledgements

The research was supported by the project PB-98-0668-C02-01 of the Dirección General de Investigación. This paper greatly benefited from the reviews of Journal referees, Dr. Ildefonso Armenteros, and Dr. Paul Wright and the careful editorial work of Dr. Bruce Sellwood. We thank them for their helpful suggestions and comments.

## References

- Allan, J.R., Matthews, R.K., 1982. Isotopic signatures associated with early meteoric diagenesis. *Sedimentology* 29, 797–817.  
 Alvaro, M., Capote, R., Vegas, R., 1979. Un modelo de evolución

- geotectónica para la Cadena Celtibérica. *Acta Geol. Hisp.* 14, 172–177.  
 Armenteros, I., Bustillo, M.A., Blanco, J.A., 1995. Pedogenic and groundwater processes in a closed Miocene basin (northern Spain). *Sediment. Geol.* 99, 17–36.  
 Arribas, M.E., 1986a. Petrología y análisis secuencial de los carbonatos lacustres del Paleógeno del sector N de la cuenca terciaria del Tajo. *Cuad. Geol. Iber.* 10, 295–334.  
 Arribas, M.E., 1986b. Estudio litoestratigráfico de una unidad paleógena: sector N de la Cuenca del Tajo. *Estud. Geol.* 42, 103–116.  
 Arribas, M.E., 1994. Paleogene of the Madrid Basin (northeast sector), Spain. In: Gierlowski-Kordesch, E., Kelts, K. (Eds.), *A Global Geological Record of Lake Basins*, vol. I. Cambridge Univ. Press, Madrid, pp. 255–259.  
 Arribas, J., Arribas, M.E., 1991. Petrographic evidence of different provenance in two alluvial fan systems (Paleogene of the northern Tajo Basin, Spain). *Geol. Soc. Spec. Publ.* 57, 263–271.  
 Arribas, M.E., Bustillo, M.A., 1985. Modelos de silicificación en los carbonatos lacustre-palustres del Paleógeno del borde NE de la Cuenca del Tajo. *Bol. Geol. Min.* 96, 325–343.  
 Arribas, M.E., Díaz-Molina, M., López-Martínez, N., Portero, J.M., 1983. El abanico aluvial paleógeno de Beleña de Sorbe (Cuenca del Tajo): facies, relaciones espaciales y evolución. X Congreso Nacional de Sedimentología, Menorca. Comunicaciones, vol. 1, pp. 34–38.  
 Borthwick, J., Harmon, R.S., 1982. A note regarding ClF3 as an alternative to BrF5 for oxygen isotope analysis. *Geochim. Cosmochim. Acta* 46, 1665–1668.  
 Bustillo, M.A., 2001. Cherts with moganite in continental Mg–clay deposits: an example of false Magadi-type cherts Madrid Basin, Spain. *J. Sediment. Res.* 71, 436–443.  
 Bustillo, M.A., Arribas, M.E., Pozo, M., Casas, J., 1998. Dolomitization, silicification and neof ormation of clays in lacustrine–palustrine sequences (Paleogene of the Madrid Basin, NE sector, Spain). 15th International Sedimentological Congress. IAS, Alicante, Spain, pp. 219–220.  
 Camoin, G., Casanova, J., Rouchy, J.M., Blanc-Valleron, M.M., Deconinck, J.F., 1997. Environmental controls on perennial and ephemeral carbonate lakes: the central palaeo-Andean Basin of Bolivia during Late Cretaceous to early Tertiary times. *Sediment. Geol.* 113, 1–26.  
 Casanova, C., Hillarie-Marcel, C., 1992. Chronology and paleohydrology of Late Quaternary high levels in the Manyara Basin (Tanzania) from isotopic data ( $^{12}\text{C}$ ,  $^{18}\text{O}$ ,  $^{14}\text{C}$  U/Th) on fossil stromatolites. *Quat. Res.* 38, 1–22.  
 Chafetz, H.D., 1994. Bacterially induced precipitates of calcium carbonate and lithification of microbial mats. In: Krumbein, W., Patterson, M.D., Stal, J.L. (Eds.), *Sediment Stabilization. Bibliothek und Informat Der Univ., Oldenburg*, pp. 149–163.  
 Clayton, R.N., Mayeda, T.K., 1963. The use of bromine pentafluoride in the extraction of oxygen from oxides and silicates for isotopic analysis. *Geochim. Cosmochim. Acta* 27, 43–52.  
 Clayton, R.N., O'Neil, J., Mayeda, T.K., 1972. Oxygen isotope exchange between quartz and water. *J. Geophys. Res.* 77, 3057–3067.  
 Craig, H., 1957. Isotopic standards for carbon and oxygen and

- correction factors for mass-spectrometric analysis of carbon dioxide. *Geochim. Cosmochim. Acta* 12, 133–149.
- Craig, H., 1965. The measurement of oxygen isotope paleotemperatures. In: Tongiorgi, E. (Ed.), *Stable Isotopes in Oceanographic Studies and Paleotemperatures*. Consiglio Nazionale delle Ricerche, Laboratorio di Geologia Nucleare, Pisa, pp. 161–182.
- Craig, H., Gordon, L.I., 1965. Deuterium and oxygen-18 variations in the ocean and the marine atmosphere. In: Tongiorgi, E. (Ed.), *Stable Isotopes in Oceanographic Studies and Paleotemperatures*. Consiglio Nazionale delle Ricerche, Laboratorio di Geologia Nucleare, Pisa, pp. 9–130.
- Degens, E.T., Epstein, S., 1964. Oxygen and carbon isotope ratios in coexisting calcites and dolomites from recent and ancient sediments. *Geochim. Cosmochim. Acta* 28, 23–44.
- Epstein, S., Buchsbaum, R., Lowenstam, H.A., Urey, H., 1953. Revised carbonate–water isotopic temperature scale. *Geol. Soc. Am. Bull.* 64, 1315–1326.
- Epstein, S., Graf, D.L., Degens, E.T., 1964. Oxygen isotope studies on the origin of dolomites. In: Craig, H. (Ed.), *Isotopic in Cosmic Chemistry*. North-Holland, Amsterdam, pp. 169–180.
- Eugster, H.P., Kelts, K., 1983. Lacustrine chemical sediments. In: Goudie, A.S., Pye, K. (Eds.), *Chemical Sediments and Geomorphology*, Academic Press, London, pp. 321–368.
- Fontes, J.Ch., Fritz, P., Létolle, R., 1970. Composition isotopique, minéralogique et genèse des dolomies du Bassin de Paris. *Geochim. Cosmochim. Acta* 34, 279–294.
- Freytet, P., Plaziat, J.C., 1982. Continental carbonate sedimentation and pedogenesis—late cretaceous and early tertiary of Southern France. *Contrib. Sedimentol.* 12, 213 pp.
- Friedman, I., Gleason, J.D., 1973. Notes on the bromine pentafluoride technique of oxygen extraction. *J. Res. U.S. Geol. Surv.* 1, 679–680.
- Fritz, P., Smith, D.G.W., 1970. The isotopic composition of secondary dolomites. *Geochim. Cosmochim. Acta* 34, 1161–1173.
- Gasse, F., Fontes, J.C., Plaziat, J.C., Carbonel, P., Kaczmarek, I., De Deckker, P., Soulie-Marsche, I., Callot, I., Dupeuble, P.A., 1987. Biological remains, geochemistry and stable isotopes for the reconstruction of environmental and hydrological changes in the Holocene lakes from North Sahara. *Palaeogeogr. Palaeoclimatol. Palaeoecol.* 60, 1–46.
- Gérdes, G., Krumbein, W.E., Reineck, H.-E., 1994. Microbial mats as architects of sedimentary surface structures. In: Krumbein, W., Patterson, M.D., Stal, J.L. (Eds.), *Sediment Stabilization. Bibliothek und Inform. der Univ., Oldenburg*, pp. 165–181.
- Geyh, H., Merkt, J., Müller, H., 1971. Sediment, pollen and isotopopenalysen und jahreszeitlich geschichteten Ablagerungen in zentralen Teil des Schleinsees. *Arch. Hydrobiol.* 69, 366–399.
- Gierlowski-Kordesch, E., Kelts, K., 1994. *Global Geological Record of Lake Basins*, vol. 1. Cambridge Univ. Press, Cambridge, 427 pp.
- Grigor'ev, D.P., 1965. *Ontogeny of Minerals: Translated from Russian, Israel Program for Scientific Translation, Jerusalem*, 250 pp.
- Gunatilaka, A., 1991. Dolomite formation in coastal Al-Khiran, Kuwait Arabian Gulf—a re-examination of the sabkha model. *Sediment. Geol.* 72, 35–53.
- Hardy, R., Tucker, M., 1988. X-ray powder diffraction of sediments. In: Tucker, M. (Ed.), *Techniques in Sedimentology*. Blackwell, Oxford, pp. 191–228.
- Hesse, R., 1990. Silica diagenesis: origin of inorganic and replacement cherts. In: McIlreath, A., Morrow, D.W. (Eds.), *Diagenesis*. Geoscience of Canada, vol. 4, GAC, Canada, pp. 253–275.
- Hudson, J.D., 1977. Stable isotopes and limestone lithification. *J. Geol. Soc. (London)* 133, 637–660.
- Jones, B., Renaut, R.W., Rosen, M.R., Klyen, L., 1998. Primary siliceous rhizoliths from Loop Road hot springs, North Island, New Zealand. *J. Sediment. Res.* 68, 115–123.
- Keith, M.L., Weber, J.N., 1964. Carbon and oxygen composition of selected limestones and fossils. *Geochim. Cosmochim. Acta* 28, 1787–1816.
- Kelts, K., Hsü, K.J., 1978. Freshwater carbonate sedimentation. In: Lerman, A. (Ed.), *Lakes, Chemistry, Geology Physics*. Springer-Verlag, Berlin, pp. 295–353.
- Kolodny, Y., Epstein, S., 1976. Stable isotope geochemistry of deep-sea cherts. *Geochim. Cosmochim. Acta* 40, 1195–1209.
- Krenmayr, H.G., 1997. Chalk and delta sediments from the last interglacial at Mondsee (Upper Austria). 18th IAS Regional European Meeting of Sedimentology, IAS, Heidelberg, pp. 208–209.
- Land, L.S., 1980. The isotopic and trace element geochemistry of dolomite: the state of the art. In: Zenger, D.H., Dunham, J.B., Ethington, R.L. (Eds.), *Concepts and Models of Dolomitization*. Soc. Econ. Paleont. Miner., Spec. Public., vol. 28. SEPM, Tulsa, Oklahoma, pp. 87–110.
- Land, L.S., 1983. The application of stable isotopes to the studies of the origin of dolomite and to problems of diagenesis of clastic sediments. In: Arthur, M.A., Anderson, T.F. (Eds.), *Stable Isotopes in Sedimentary Geology*. SEPM Short Course, vol. 10, pp. 4.1–4.22.
- Last, W.M., 1990. Lacustrine dolomite—an overview of modern, Holocene, and Pleistocene occurrences. *Earth-Sci. Rev.* 27, 221–263.
- Lumsden, D.L., 1979. Discrepancy between thin section and X-ray estimates of dolomite in limestone. *J. Sediment. Petrol.* 49, 429–436.
- Lumsden, D.N., Chimahusky, J.S., 1980. Relationship between dolomite nonstoichiometry and carbonate facies parameters. In: Zenger, D.H., Dunham, J.B., Ethington, R.L. (Eds.), *Concepts and Models of Dolomitization*. Soc. Econ. Paleont. Miner., Spec. Public., vol. 28. SEPM, Tulsa, Oklahoma, pp. 123–137.
- Maliva, R., Siever, R., 1988. Pre-Cenozoic nodular cherts: evidence for opal-CT precursors and direct quartz replacement. *Am. J. Sci.* 288, 799–809.
- Matheney, R.K., Knauth, L.P., 1993. New isotopic temperature estimates for early silica diagenesis in beaded cherts. *Geology* 21, 519–522.
- Matthews, A., Katz, A., 1977. Oxygen isotope fractionation during the dolomitization of calcium carbonate. *Geochim. Cosmochim. Acta* 41, 1431–1438.
- McBride, E.F., Abdel-Wahab, A., El-Younsy, A.M., 1999. Origin of spheroidal chert nodules, Drunka Formation (Lower Eocene), Egypt. *Sedimentology* 46, 733–755.
- McCrea, J.M., 1950. On the isotopic chemistry of carbonates and a paleotemperature scale. *J. Chem. Phys.* 18, 849–857.
- McKenzie, J.A., 1981. Holocene dolomitization of calcium carbo-

- nate sediments from the coastal sabkhas of Abu Dhabi, U.A.E.: a stable isotope study. *J. Geol.* **89**, 185–198.
- Murata, K.J., Norman, M.B., 1976. An index of crystallinity for quartz. *Am. J. Sci.* **276**, 1120–1130.
- Müller, G., Wagner, F., 1978. Holocene carbonate evolution of Lake Balaton (Hungary): a response to climate and the input of man. In: Matter, A., Tucker, M.E. (Eds.), *Modern and Ancient Lake Sediments*. Spec. Publ. Int. Ass. Sedimentology, vol. 2. IAS, Oxford, pp. 57–81.
- Müller, G., Iron, G., Förstner, U., 1972. Formation and diagenesis of inorganic Ca–Mg carbonates in the lacustrine environment. *Naturwissenschaften* **59**, 158–164.
- Northrop, D.A., Clayton, R.N., 1966. Oxygen isotope fractionation in systems containing dolomite. *J. Geol.* **74**, 174–196.
- Neil, J., Epstein, S., 1966. Oxygen isotope fractionation in the system dolomite–calcite–carbon dioxide. *Science* **152**, 198–201.
- Platt, N.H., Wright, V.P., 1991. Lacustrine carbonates: facies models, facies distributions and hydrocarbon aspects. Spec. Publ. Int. Assoc. Sedimentol. **13**, 57–74.
- Riding, R.E., 1994. Stromatolite survival and change: the significance of Shark Bay and Lee Stocking Island subtidal columns. In: Krumbein, W.E., Paterson, D.M., Stal, L.J. (Eds.), *Biostabilization of Sediments*. Bibliotheks und Informationssystem der Universität, Oldenburg, pp. 183–202.
- Salomons, W., Mook, W.G., 1976. Isotope geochemistry of carbonate dissolution and reprecipitation in soils. *Soil Sci.* **122**, 15–24.
- Salomons, W., Goudie, A., Mook, W.G., 1978. Isotopic composition of calcrete deposits from Europe, Africa and India. *Earth Surf. Processes* **3**, 43–57.
- Spiker, E.C., 1980. Carbon isotopes as indicators of the source and fate of carbon in rivers and estuaries. In: *Flux of Organic Carbon by Rivers to the Oceans*, U.S. Dept. of Energy, Office of Energy Research, CONF-8009140, UC-11, pp. 75–108.
- Talbot, M.R., 1990. A review of the palaeohydrological interpretation of carbon and oxygen isotopic ratios in primary lacustrine carbonates. *Chem. Geol.* **80**, 261–279.
- Talbot, M.R., Kelts, K., 1990. Paleolimnological signatures from carbon and oxygen isotopic ratios in carbonates from organic carbon-rich lacustrine sediments. In: Katz, B.J. (Ed.), *Lacustrine Basin Exploration—Case Studies and Modern Analogs*. Mem. Am. Assoc. Pet. Geol., vol. 50, AAPG, Tulsa, Okla., pp. 99–112.
- Talma, A.S., Netterberg, F., 1983. Stable isotopic abundances in calcretes. In: Wilson, R.C.L. (Ed.), *Residual Deposits: Surface Related Weathering Processes and Materials*. Spec. Publ. Geol. Soc. London, vol. 11, Geological Society, London, pp. 221–233.
- Tucker, M.E., Wright, V.P., 1990. *Carbonate Sedimentology*. Blackwell, Oxford, 482 pp.
- Winsborough, B.M., 2000. Diatoms and benthic microbial carbonates. In: Riding, R.E., Stanley, M.A. (Eds.), *Microbial Sediments*. Springer-Verlag, Berlin, pp. 76–83.
- Wright, V.P., Alonso-Zarza, A., Sanz, M.E., Calvo, J.P., 1997. Diagenesis of late Miocene micritic lacustrine carbonates, Madrid Basin, Spain. *Sediment. Geol.* **114**, 81–95.
- Yébenes, A., de la Peña, J.A., Ordoñez, S., 1973. Sedimentos dolomíticos para-actuales: la “Tierra Blanca” de la Roda (Albacete). *Estud. Geol.* **29**, 343–349.
- Zijlstra, H., 1995. *The sedimentology of chalk*. Lecture Notes in Earth Sciences. Springer-Verlag, Berlin.
- Zuffa, G.G., 1980. Hybrid arenites: their composition and classification. *J. Sediment. Petrol.* **50**, 21–29.